

## Article

# Spatiotemporal Evolution of Wind Erosion and Ecological Service Assessments in Northern Songnen Plain, China

Jixian Mo <sup>1,2</sup> , Jie Li <sup>2</sup>, Ziyang Wang <sup>1</sup>, Ziwei Song <sup>2</sup>, Jingyi Feng <sup>1</sup>, Yanjing Che <sup>1</sup>, Jiandong Rong <sup>3</sup> and Siyu Gu <sup>1,\*</sup>

<sup>1</sup> College of Resources and Environment, Northeast Agricultural University, Harbin 150030, China; mojixian8208@sina.com (J.M.); wangziying0929@126.com (Z.W.); sdaufjy2018@163.com (J.F.); 17863527374@163.com (Y.C.)

<sup>2</sup> College of Life Science and Agriculture and Forestry, Qiqihar University, Qiqihar 161006, China; joycelepp@163.com (J.L.); syh20100511@sina.com (Z.S.)

<sup>3</sup> Qiqihar Experimental Station, Heilongjiang Province Hydraulic Research Institute, Qiqihar 161006, China; rjd221@126.com

\* Correspondence: gusiyu@neau.edu.cn; Tel.: +86-136-5468-8577

**Abstract:** The northern Songnen Plain in China is one of the most important areas for grain production in China, which has been increasingly affected by wind erosion in recent years. This study analyzed the dynamic spatiotemporal distribution of wind erosion in the northern Songnen Plain from 2010 to 2018 using the Revised Wind Erosion Equation model. The ecological service function of the study area was evaluated by constructing a spatial visualization map of windbreak and sand-fixation service flow. Wind erosion worsened from 2010 to 2018. The gravity center of different categories of wind erosion intensity moved to the northeast, indicating a risk of spreading from south to north. The amount of wind erosion in 2018 increased by 50.78% compared with 2010. The increase of wind force and temperature and the decrease of precipitation may have contributed to these trends. Long-term wind erosion led to soil coarsening, decreased soil organic matter, soil organic carbon, and total nitrogen contents, and increased soil CaCO<sub>3</sub> and pH, which may be one reason for slight soil salinization observed in some regions. Therefore, windbreak and sand-fixation management and eco-environmental protection are urgently required. This study is the first detailed assessment of wind erosion in the northern Songnen Plain on a regional scale and the first to propose measures for ecological restoration and desertification control.

**Keywords:** wind erosion; dynamic process; spatiotemporal distribution; ecological effects; sustainable management



**Citation:** Mo, J.; Li, J.; Wang, Z.; Song, Z.; Feng, J.; Che, Y.; Rong, J.; Gu, S. Spatiotemporal Evolution of Wind Erosion and Ecological Service Assessments in Northern Songnen Plain, China. *Sustainability* **2023**, *15*, 5829. <https://doi.org/10.3390/su15075829>

Academic Editor: Grigorios L. Kyriakopoulos

Received: 31 January 2023

Revised: 25 March 2023

Accepted: 26 March 2023

Published: 27 March 2023



**Copyright:** © 2023 by the authors. Licensee MDPI, Basel, Switzerland. This article is an open access article distributed under the terms and conditions of the Creative Commons Attribution (CC BY) license (<https://creativecommons.org/licenses/by/4.0/>).

## 1. Introduction

Wind erosion is a phenomenon of soil erosion, which refers to the process of topsoil being eroded and carried away by the action of wind [1]. Wind erosion causes the loss of soil clay, silt, and nutrients, leading to the change of soil texture and hence to desertization [2]. Wind erosion causes many crop losses, which severely threatens agricultural production and food security [3]. In addition, wind erosion can also cause sandstorms, which pollute the atmospheric environment and endanger human health [4]. According to the United Nations Environment Program (UNEP) statistics, the area of global soil degradation caused by wind erosion is about  $5.48 \times 10^6$  km<sup>2</sup>, accounting for 46.4% of the degraded soil [5,6]. The wind erosion area in China has reached  $1.61 \times 10^6$  km<sup>2</sup> [7], which has become a considerable threat to ecological security and sustainable socio-economic development. Therefore, it is crucial to assess the regional wind erosion intensity and dynamic process to provide a basis for predicting the wind erosion development trend and carrying out desertization control.

The Songnen Plain is located in the western regions of Jilin Province and Heilongjiang Province in northeast China, with an area of  $18.3 \times 10^4$  km<sup>2</sup> [8]. As one of the most

important areas for food production in China, the Songnen Plain has experienced an extensive land use transformation in the past few decades [9]. A large amount of land has been reclaimed into farmland [10], which has contributed to ensuring the national grain output. However, the average annual precipitation in the Songnen Plain is only 350–450 mm [11,12]. Frequent and robust monsoons make the area vulnerable to wind erosion [13], and desertization has occurred in some areas to varying degrees. In recent years, wind erosion in the Songnen Plain showed an increasing trend [14]. Wind erosion in the Songnen Plain has accounted for 21–33% of the total soil erosion, reaching an erosion rate of 2.22 mm/a [15]. Since the mid-1980s, the sandy land in the Songnen Plain has increased by 0.44% per year [16]. By the end of the 20th century, the sandy land area in the Songnen Plain reached  $5.96 \times 10^4$  km<sup>2</sup> [10], becoming the fifth largest sandy land in China [17]. In addition, the Songnen Plain is next to the Horqin Sandy Land in the south and the Hulun Buir Sandy Land in the northwest [18]. The wind erosion formed in these areas lasts for a long time and has a significant intensity [17], which may be one reason for desertization in the Songnen Plain. However, wind erosion in the Songnen Plain has not attracted enough attention [19]. The research on soil erosion still focuses on water erosion [9,20] and freeze–thaw erosion [21,22]. Therefore, assessing the wind erosion in the Songnen Plain is extremely important to understand the distribution types of soil erosion in the grain-producing areas of northeast China and to plan reasonable soil erosion control strategies.

A detailed evaluation of wind erosion is essential to adopt appropriate measures of prevention and control. The Revised Wind Erosion Equation (RWEQ) model has been widely used to analyze the spatiotemporal distribution characteristics and dynamic change trend of wind erosion at various scales [1,6,9,23–25]. In recent years, the application of the RWEQ model to large-scale regional wind erosion research in northern China has been pervasive [6,17,26], which provides a basis for clarifying the distribution of global wind erosion. Further clarifying the detailed spatiotemporal distribution and dynamic process of wind erosion in small-scale areas is a prerequisite for formulating and implementing precise wind erosion control measures. However, most studies focused on sandy lands, grasslands, and plateau areas, such as Inner Mongolia grasslands [27], Horqin sandy land [4], and the Mongolian plateau [23]. The study of wind erosion in the Songnen Plain mainly focused on the south area adjacent to the Horqin sandy land [4,28]. In contrast, the wind erosion situation in the north area still needs comprehensive and systematic evaluation. There is a lack of scientific and systematic research on the classification, distribution, diffusion trends, migration paths, and ecological effects of wind erosion in the northern Songnen Plain. Therefore, it is urgent to conduct a comprehensive study on the spatiotemporal dynamic changes of wind erosion and ecological services in the northern Songnen Plain to plan accurate windbreak and sand-fixation strategies. Our research objectives were: (1) to comprehensively analyze the spatiotemporal distribution and dynamic process of wind erosion in the northern Songnen Plain from 2010 to 2018; (2) to evaluate the ecological effects and influencing factors of wind erosion; and (3) to develop a spatial visualization of windbreak and sand-fixation service flow and assess the service function of the ecosystem windbreak and sand-fixation in the study area. The research results can provide a basis for improving the ecological environment and sustainable development in the Songnen Plain.

## 2. Materials and Methods

### 2.1. Study Area

The northern Songnen Plain is located in the west of Heilongjiang Province (45°52' N–48°32' N, 122°24' E–125°20' E) (Figure 1), adjacent to the north edge of Horqin Sandy Land. It is a part of Heilongjiang New Economic Industrial Park—“Ha-Da-qi Industrial Corridor”. The study area covers Qiqihar City, Lindian County, and Durbert Mongolian Autonomous County, with a total area of  $3.85 \times 10^4$  km<sup>2</sup>, and is mainly planted with corn and rice. The most widely distributed soil types of the area are chernozem and aeolian sandy soil according to the FAO world classification system. The study area has a semi-arid

low temperature continental-monsoon climate, with an annual rainfall of 350–450 mm and annual average temperature of 3.6 °C [11,12]. The period from June to August accounts for more than 70% of the total rainfall [29]. The annual potential evapotranspiration (PET) exceeds 1000 mm, and the ratio of annual precipitation to PET is as low as 0.2–0.5 [30]. Gale weather occurs on 10–30 days yearly, mainly in spring and autumn. According to the land use type and accessibility, a field survey was conducted in the spring of 2022, and 56 soil samples (0–10 cm) were collected for subsequent trend analysis.

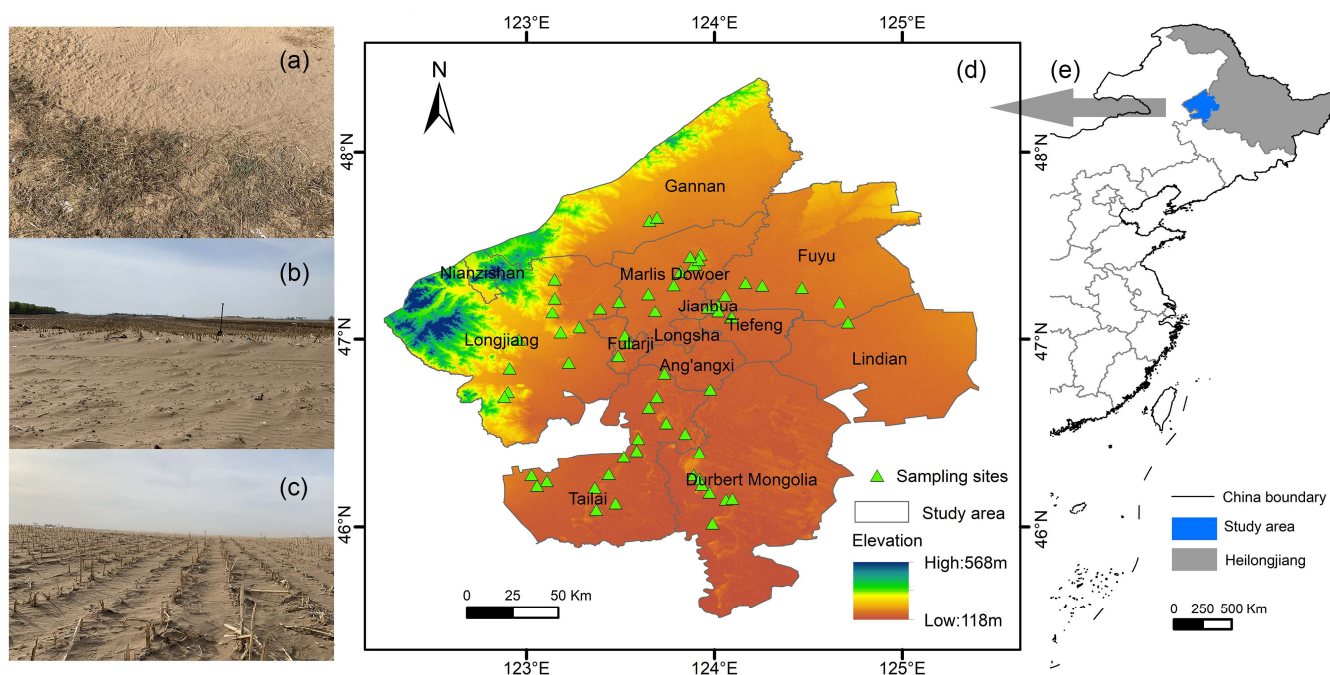


**Figure 1.** Study area. (a–c) Landscapes with typical wind erosion; (d) distribution of sampling sites; (e) geographical position of the study.

## 2.2. Workflow and Data Sources

Figure 2 shows the workflow of wind erosion research in the northern Songnen Plain. First, based on meteorological data, soil properties, and vegetation coverage, the RWEQ model was used to calculate the amounts of wind erosion in 2010, 2014, and 2018 and then to analyze the spatiotemporal distribution of wind erosion and the migration path of wind erosion gravity center. Second, the collected soil samples were analyzed to clarify wind erosion's ecological effect on the soil's physicochemical properties. Third, the influence of wind force ( $W_f$ ), precipitation, and temperature ( $T$ ) on wind erosion was analyzed using the constraint line method. Finally, the supply rate and demand degree of the ecosystem windbreak and sand-fixation service flow were analyzed comprehensively to promote the sustainable management of the agricultural eco-environment in the study area.

The meteorological data came from the daily value data set (V3.0) of China's surface climate data with a 3-h temporal and 0.1° spatial resolution (<http://data.cma.cn>, accessed on 4 April 2022)). The temperature unit is the thermodynamic temperature K. Snow data (mm) were derived from the long-term data set of daily snow depth in China with a 1-day temporal and 25 km spatial resolution (<http://data.tpdc.ac.cn>, accessed on 6 April 2022). Soil property data were derived from the Soil Map Based Harmonized World Soil Database (HWSD, v1.1) with a 1 km spatial resolution (<http://data.casnw.net/portal/>, accessed on 6 April 2022). To obtain a 250 m × 250 m resolution, each original 1 km<sup>2</sup> pixel point was divided into 16 parts and the 16 new pixel points were subject to interpolation according to the original soil data values (HWSD, v1.1) around these pixel points. These values were used for the RWEQ model, whereas the data from the 56 soil samples were used for the analysis presented in 3.3 ecological effects. Elevation data were derived from a digital

elevation model (DEM) data with a spatial resolution of 30 m (<http://www.gscloud.cn>, accessed on 7 April 2022). The Normalized Difference Vegetation Index (NDVI) data came from the National Aeronautics and Space Administration (NASA) Land Topical Product MOD13Q1 with a 16-day temporal and 250 m spatial resolution (<https://ladsweb.modaps.eosdis.nasa.gov>, accessed on 7 April 2022). The ECMWF Re-Analysis (ERA) data were derived from the European Centre for Medium-Range Weather Forecasts with a 3-h temporal and 0.75° spatial resolution (<https://www.ecmwf.int>, accessed on 9 April 2022). All the data were converted to a 250 m spatial resolution using ArcMap (v10.8) to calculate the wind erosion modulus.

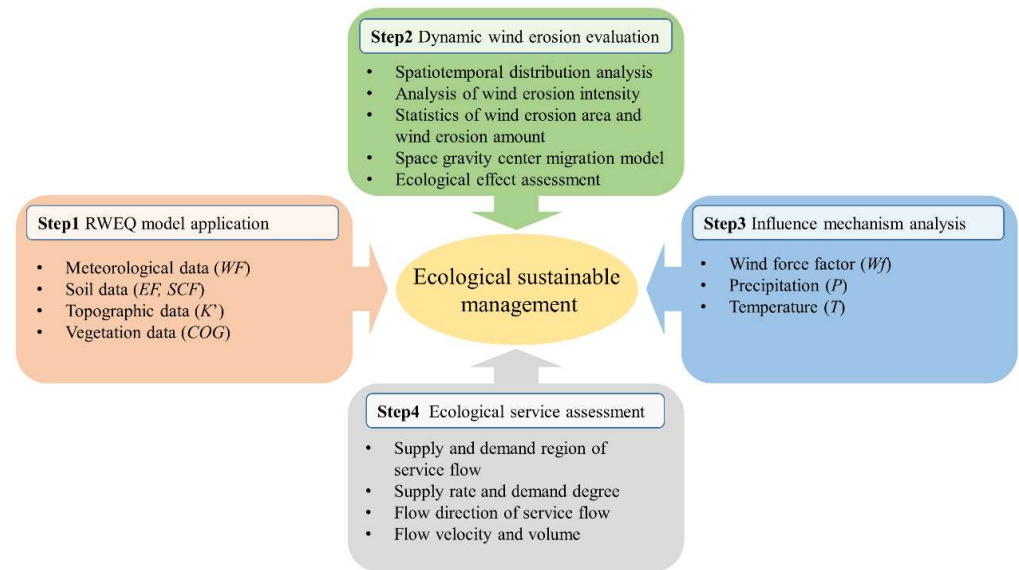


**Figure 2.** Workflow of wind erosion research in the northern Songnen Plain.

### 2.3. RWEQ Model

The RWEQ model calculates the study area's actual and potential wind erosion amount. Potential wind erosion refers to wind erosion without vegetation on the ground. The difference between the actual and potential wind erosion amount is the service function of windbreak and sand-fixation [24,31]. The calculation equation is described as below:

$$D = SL_p - SL_a \quad (1)$$

$$SL_p = \left(2 \times z / S_p^2\right) \times Q_{pmax} \times e^{-(z/S_p)^2} \quad (2)$$

$$Q_{pmax} = 109.8 \times (WF \times EF \times SCF \times K') \quad (3)$$

$$S_p = 150.71 \times (WF \times EF \times SCF \times K')^{-0.3711} \quad (4)$$

$$SL_a = \left(2 \times z / S_a^2\right) \times Q_{amax} \times e^{-(z/S_a)^2} \quad (5)$$

$$Q_{amax} = 109.8 \times (WF \times EF \times SCF \times K' \times COG) \quad (6)$$

$$S_a = 150.71 \times (WF \times EF \times SCF \times K' \times COG)^{-0.3711} \quad (7)$$

where  $D$  is the reduced amount of wind erosion ( $\text{kg}/\text{m}^2$ ).  $z$  represents the downwind distance (m), which is a constant of 100 in this study [32].  $SL_p$  and  $SL_a$  are potential wind

erosion and actual wind erosion ( $\text{kg}/\text{m}^2$ ), respectively, representing the maximum soil loss without vegetation cover and the actual soil loss with vegetation cover.  $Q_{pmax}$  and  $Q_{amax}$  represent the maximum sand transport capacity of potential wind force and current actual wind force ( $\text{kg}/\text{m}$ ), respectively.  $S_p$  and  $S_a$  are the lengths of key plots (m), that is, the length of the plots whose soil transport capacity reaches 63.2% of the maximum transport capacity ( $Q_{max}$ ).  $WF$  is a meteorological factor ( $\text{kg}/\text{m}$ ), which represents the ability of wind to transport soil particles under the influence of rainfall, temperature, radiation, and snow cover.  $EF$  is the soil erodibility factor, which refers to the sensitivity of soil to wind erosion. The lower the content of organic matter and the smaller the particle size, the greater the soil erodibility and the easier it is to be eroded.  $SCF$  is the soil crust coefficient, representing the micro-layer that can resist wind erosion formed by the interaction between some substances and the soil surface.  $K'$  denotes the surface roughness factor, which refers to the influence of soil surface roughness caused by the terrain on wind erosion.  $COG$  is the vegetation coverage factor, which represents the inhibition of vegetation coverage on wind erosion. Detailed calculation methods for these parameters are described in previous literature [33,34]. Note that  $WF$  must be calculated using the wind speed at the height of 2 m to satisfy the assumptions of the RWEQ model [1]. The  $WF$  here is converted from the wind speed at a 10 m height by using the wind profile equation as follows:

$$U_2 = U_{10} \times (h_2/h_{10})^{1/7} \quad (8)$$

where  $U_2$  and  $U_{10}$  represent the wind speed (m/s) at the height of 2 m ( $h_2$ ) and 10 m ( $h_{10}$ ), respectively.

#### 2.4. Analytical Methods

##### 2.4.1. Wind Erosion Gravity Center and Migration

In geography, the variation in the geographical gravity center can reflect the change in the degree and trend of geographical phenomena [35]. The migration direction and distance reflect the changing trend and range of spatiotemporal distribution, respectively. This study uses the gravity center model of migration to calculate the gravity center of wind erosion, which can reveal the variation of the wind erosion spatiotemporal distribution characteristics in the study area [27,36]. The calculation equation of gravity center is as follows:

$$X_t = \sum_{i=1}^n (C_{ti} \times x_{ti}) / \sum_{i=1}^n C_{ti} \quad (9)$$

$$Y_t = \sum_{i=1}^n (C_{ti} \times y_{ti}) / \sum_{i=1}^n C_{ti} \quad (10)$$

where  $X_t$  and  $Y_t$  are the longitude and latitude coordinates of gravity center in the  $t$ -th year.  $C_{ti}$  and  $n$  are the areas of the  $i$ -th polygon and the polygon amount of the same wind erosion intensity in the year  $t$ , respectively.  $x_{ti}$  and  $y_{ti}$  are the longitude and latitude coordinates of  $C_{ti}$ .

The spatial movement of the gravity center between two years is calculated as follows [37]:

$$D_{s-f} = C \times \sqrt{(Y_s - Y_f)^2 + (X_s - X_f)^2} \quad (11)$$

where  $D_{s-f}$  represents the moving distance of a wind erosion gravity center between two years ( $s$  and  $f$ ).  $C$  is the conversion coefficient between the geographic coordinate and the planar distance, and the value in this study is 111.111 km. The terms  $(X_s, Y_s)$  and  $(X_f, Y_f)$  represent the longitude and latitude coordinates of the gravity center of two different years, which are calculated from Equations (9) and (10).

##### 2.4.2. Trend Analysis

The linear trend means that a phenomenon shows a stable linear change rule with time [26], and linear trend analysis (LTA) is a method to quantify this linear change rule.

This study uses the LTA method to analyze the wind erosion change trend of the 56 soil sample sites (pixel) from 2010 to 2018. We compared the soil samples collected from the sampling sites of increased wind erosion with those collected from the sampling sites of decreased wind erosion to clarify the response of soil physical and chemical properties to wind erosion using the equation:

$$\alpha = \left( \left( t \times \sum_{n=1}^t (n \times x_n) \right) - \left( \sum_{n=1}^t n \right) \times \left( \sum_{n=1}^t x_n \right) \right) / \left( \left( t \times \sum_{n=1}^t n^2 \right) - \left( \sum_{n=1}^t n \right)^2 \right) \quad (12)$$

where  $t$  represents the  $t$ -th year within the research period;  $x_n$  is the wind erosion amount of a quadrat (or soil sample site) in the  $t$ -th year.  $\alpha > 0$  indicates a trend of wind erosion increasing in the quadrat (or soil sample site), while  $\alpha < 0$  indicates a decreased trend of wind erosion.

#### 2.4.3. Constraint Line Analysis

The layout and process of ecosystems are often affected by many factors, such as climate change and human activities. A scatter plot describing the correlation between ecosystem variables and influencing factors is usually displayed as a border scatter plot [38]. The constraint line method can effectively extract the boundary of the scatter plot, representing the constraint relationship between two variables. It provides an effective method for understanding the relationship between ecosystem variables and influencing factors. In this study, the ecological variable value range on the abscissa of the scatter chart is divided into 10 equal parts. The subsection quantile regression method plots the constraint line of wind, temperature, and rainfall response to wind erosion [39], and the 95% quantile was selected as the boundary point [38]. OriginPro 9 was used for regression analysis.

#### 2.4.4. Ecosystem Services

Ecosystem services refer to the benefits that people obtain from the products or services provided by ecosystems to humans. Forestland and grassland can decrease wind speed and fix the soil, and thus have the service function of reducing or avoiding the harmful impact of soil quality decline caused by soil erosion on humans. This service is called windbreak and sand-fixation ecosystem service [24]. The quantitative study of ecosystem services in wind erosion areas can reveal the variation trends of wind erosion, clarify the supply and demand relationship of ecosystem services, and promote the visual study on ecosystem services [40]. The vegetation-covered regions in the study area are the supply regions for windbreak and sand-fixation, while the agricultural and urban regions are the demand regions [31]. Equations are as follows:

$$\text{Supply rate(\%)} = (G / SL_p) \times 100\% \quad (13)$$

$$\text{Demand degree(\%)} = (SL_a / SL_p) \times 100\% \quad (14)$$

where the supply rate and demand degree represent the supply rate of windbreak and sand-fixation service supply regions and the demand degree of windbreak and sand-fixation services demand regions, respectively.

This study takes the wind direction as the flow direction of windbreak and sand-fixation service. Since most of the wind erosion in the northern Songnen Plain occurs in spring, the average wind direction in the spring of 2010, 2014, and 2018 is taken as the flow direction of windbreak and sand-fixation services. Similarly, the wind speed and sand-fixation amount characterize the windbreak and sand-fixation service's flow rate and volume, respectively. The service flow was visualized on ArcMap.

### 3. Results

The study area is located in Northeast China. In winter, thick snow prevents wind erosion in the study area. Therefore, this study did not count wind erosion in winter

(December to February) but only assessed wind erosion in spring, summer, and autumn for nine months [41]. In order to clarify the difference in wind erosion in different years, this study assessed the wind erosion at four-year intervals, namely in 2010, 2014, and 2018.

### 3.1. Spatiotemporal Distribution Characteristics of Wind Erosion

Figure 3 shows the spatiotemporal distribution of wind erosion in spring, summer, and autumn of 2010, 2014, and 2018 using the spatial resolution of  $250\text{ m} \times 250\text{ m}$  (thus a total of 618,779 pixels, each with a surface of 6.25 ha, are used). Table 1 shows the wind erosion amount and average wind erosion intensity of each administrative region in the northern Songnen Plain. The regions with high wind erosion intensity are distributed in the south and southeast of the study area. In contrast, the north and northeast regions have weak wind erosion intensity. The most severe wind erosion occurs in Tailai, with an annual wind erosion amount of  $637.67 \times 10^4\text{ t}$  and an annual wind erosion intensity of 16.22 t/ha. Wind erosion was highest in southern Tailai, exceeding 30 t/ha. The average annual wind erosion amounts at regional level increased in the following order: Tailai, Durbert Mongolia, Longjiang, Lindian, Fuyu, Marlis Dawoer, Gannan, Angangxi, Tiefeng, Nianzishan, Fularji, Jianhua, and Longsha. The wind erosion intensities of Tailai, Durbert Mongolia, and Longjiang are higher than those of other regions.

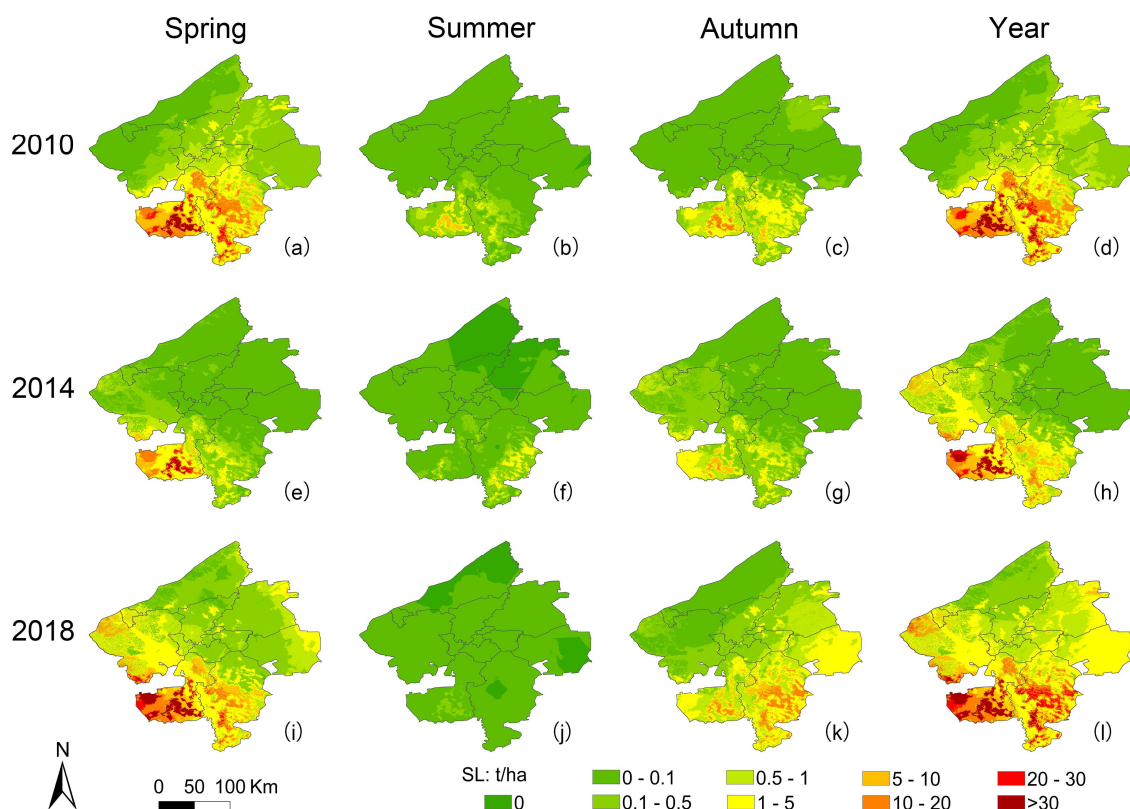


**Figure 3.** Spatiotemporal distribution characteristics of wind erosion in three seasons in 2010, 2014, and 2018. (a,e,i): March to May; (b,f,j): June to August; (c,g,k): September to November; and (d,h,l): March to November.

**Table 1.** The wind erosion amount and average wind erosion intensity of each administrative region in the northern Songnen Plain from 2010 to 2018.

| Regions          | Amount of Wind Erosion ( $10^4$ t) |        |        |        | Mean Wind Erosion Intensity (t/ha) |        |        |       |
|------------------|------------------------------------|--------|--------|--------|------------------------------------|--------|--------|-------|
|                  | Spring                             | Summer | Autumn | Year   | Spring                             | Summer | Autumn | Year  |
| Longsha          | 0.61                               | 0.01   | 0.18   | 0.79   | 0.40                               | 0.00   | 0.12   | 0.52  |
| Jianhua          | 0.73                               | 0.01   | 0.30   | 1.04   | 0.61                               | 0.00   | 0.25   | 0.86  |
| Fularji          | 2.12                               | 0.04   | 0.49   | 2.65   | 0.56                               | 0.01   | 0.13   | 0.70  |
| Nianzishan       | 3.11                               | 0.00   | 0.48   | 3.60   | 1.04                               | 0.00   | 0.16   | 1.20  |
| Tiefeng          | 3.30                               | 0.02   | 1.96   | 5.28   | 0.44                               | 0.00   | 0.26   | 0.71  |
| Angangxi         | 4.15                               | 0.08   | 1.41   | 5.64   | 0.55                               | 0.01   | 0.19   | 0.75  |
| Gannan           | 7.04                               | 0.15   | 1.42   | 8.61   | 0.15                               | 0.00   | 0.03   | 0.18  |
| Marlis Dowoer    | 6.32                               | 0.07   | 2.56   | 8.95   | 0.32                               | 0.00   | 0.13   | 0.45  |
| Fuyu             | 16.21                              | 0.22   | 11.20  | 27.62  | 0.40                               | 0.01   | 0.28   | 0.69  |
| Lindian          | 13.44                              | 0.05   | 18.65  | 32.13  | 0.38                               | 0.00   | 0.53   | 0.92  |
| Longjiang        | 83.37                              | 0.39   | 11.02  | 94.78  | 1.41                               | 0.01   | 0.19   | 1.60  |
| Durbert Mongolia | 232.82                             | 10.10  | 129.03 | 371.95 | 3.86                               | 0.17   | 2.14   | 6.16  |
| Tailai           | 533.89                             | 14.92  | 88.87  | 637.67 | 13.58                              | 0.38   | 2.26   | 16.22 |

### 3.2. Dynamic Variation in Wind Erosion

#### 3.2.1. Temporal Variation Characteristics

Wind erosion from March to November in 2010, 2014, and 2018 was generally on a downtrend (Figure 4d). Nevertheless, there were important seasonal differences, which is consistent with Figure 3. Specifically, the wind erosion amount increased in November 2018 (Figure 4c), reaching  $487.56 \times 10^4$  t, indicating the wind erosion in the study area expanded from spring to spring and autumn in recent years. With more rainfall and lush crop in summer, however, no wind erosion was observed. Although the monthly variation trend of wind erosion was similar, the wind erosion amount was unstable, showing differences among the studied years. The amounts of wind erosion in 2010, 2014, and 2018 were  $1309.05 \times 10^4$  t,  $818.68 \times 10^4$  t, and  $1973.83 \times 10^4$  t, respectively, with an average of  $1367.19 \times 10^4$  t in the three years. The amount of wind erosion in 2018 increased by 50.78% from 2010, indicating the wind erosion is increasing.

#### 3.2.2. Wind Erosion Intensity

Wind erosion intensity expresses the cumulative wind erosion amount of one quadrat per year. In this study, daily wind erosion amounts from March 1 to November 30 for the 6.25 ha quadrats were summed to get the total wind erosion amount of a year, which was classified according to the classification and grade standard of soil erosion issued by the Ministry of Water Resources of China (SL190-2007). According to this classification, wind erosion in the study area covers five grades: light, mild, moderate, strong, and very strong (Figure 5). The wind erosion modulus (t/ha·a) ranges of each grade are  $0 < \text{light} \leq 2$ ,  $2 < \text{mild} \leq 25$ ,  $25 < \text{moderate} \leq 50$ ,  $50 < \text{strong} \leq 80$ , and  $80 < \text{very strong} \leq 150$ , respectively. The results show that the study area was dominated by light and mild wind erosion in 2010, 2014, and 2018. Specifically, mild wind erosion is concentrated in the south and west regions (Longjiang, Tailai, Durbert Mongolia) and scattered in other regions (e.g., Nianzishan, Marlis Dawoer, Fuyu). Strong and very strong wind erosion is concentrated in Tailai, indicating wind erosion in this region has been intensified and prevention and control works are needed.

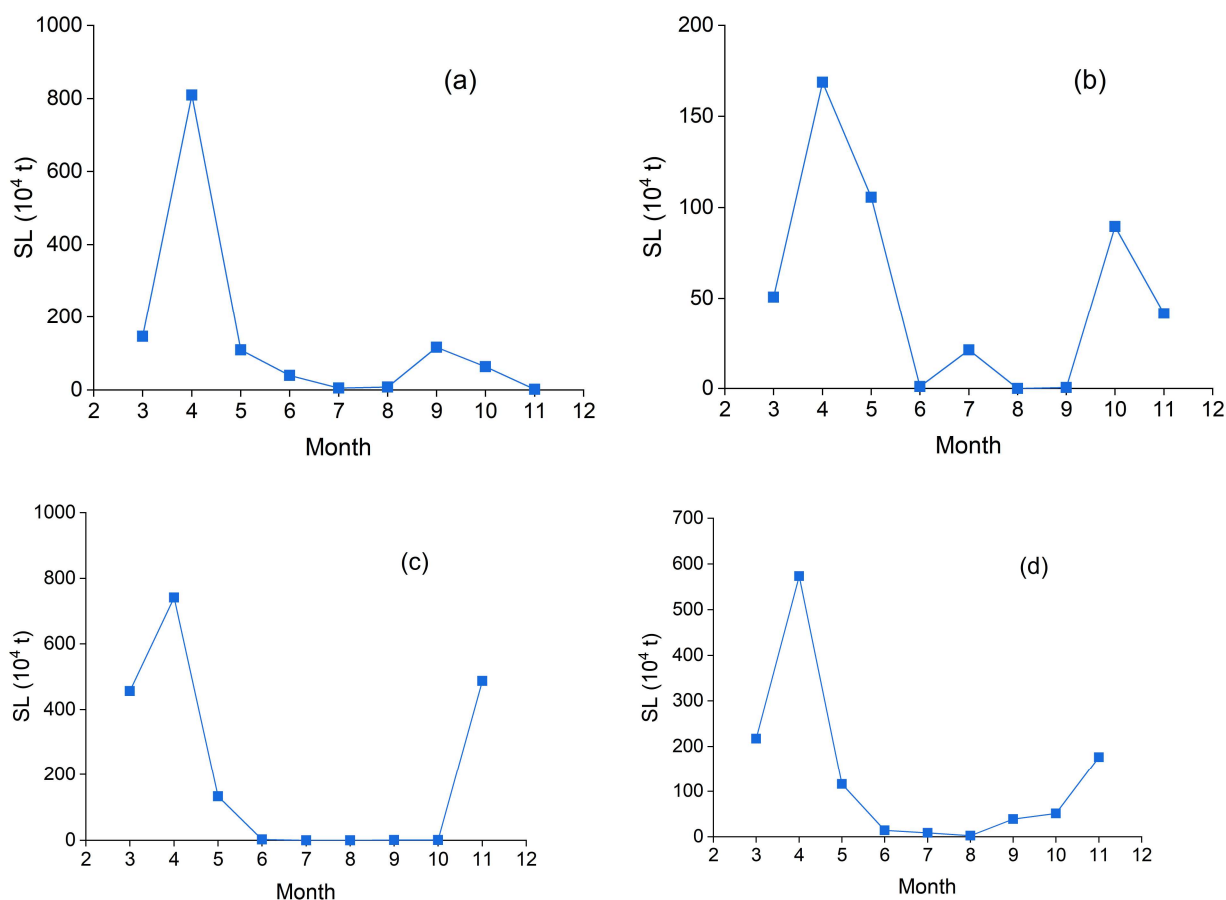


**Figure 4.** Monthly change of wind erosion amount in the northern Songnen Plain in 2010, 2014, and 2018. (a) 2010; (b) 2014; (c) 2018; and (d) three-year mean values. Here, monthly wind erosion is the sum of wind erosion of all 6.25 ha quadrats in one month. For example, the wind erosion amount in March 2010 was obtained by adding the wind erosion amount of all quadrats in the study area from March 1 to March 31, 2010.

### 3.2.3. Gravity Center Migration and Characteristics

Wind erosion grades' gravity centers (longitude and latitude coordinates) were calculated according to each 6.25 ha quadrats' longitude and latitude coordinates using Equations (9) and (10). The migration distance of the wind erosion gravity center was then calculated according to the longitude and latitude coordinates of the wind erosion gravity center in different years using Equation (11). The amount of wind erosion was then expressed as the sum of the annual wind erosion amount of all quadrats. The wind erosion area was finally calculated as the sum of all quadrats multiplied by the surface of each quadrat (i.e., 6.25 ha). Overall, wind erosion grades' gravity centers showed different migration from 2010 to 2018 (Figure 6). The gravity center of mild wind erosion has the farthest migration distance, with a cumulative migration distance of 62.57 km, followed by moderate and light wind erosion. The gravity center of mild wind erosion was initially located at the west of Durbert Mongolia, then moved 33.63 km to the northwest and 28.94 km to the northeast, and finally reached northern Tailai. It can be seen from Figure 6a that the gravity center of each wind erosion grade moved to the northeast in varying degrees. The gravity center migration distance of mild and moderate wind erosion decreased, but that of light, strong, and very strong wind erosion increased continuously (Figure 6b). In addition, except for a decrease in the area of light wind erosion (Figure 6d), the areas of wind erosion in the other four grades increased to varying degrees. Among them, the area of mild wind erosion rose by 65.27% or  $55.25 \times 10^4$  ha from 2010 to 2018. Although the area of very

strong wind erosion only increased by  $0.96 \times 10^4$  ha to  $1.84 \times 10^4$  ha, the increasing rate was up to 109.15% and mainly distributed in Tailai, further indicating that wind erosion in this region is deteriorating patterns. Although the areas of wind erosion at different grades varied with different trends from 2010 to 2018, the erosion amount of all grades of wind erosion increased (Figure 6c). The increasing amounts of wind erosion were 50.20% (light), 32.17% (mild), 77.42% (moderate), 14.74% (strong), and 65.53% (very strong), respectively.

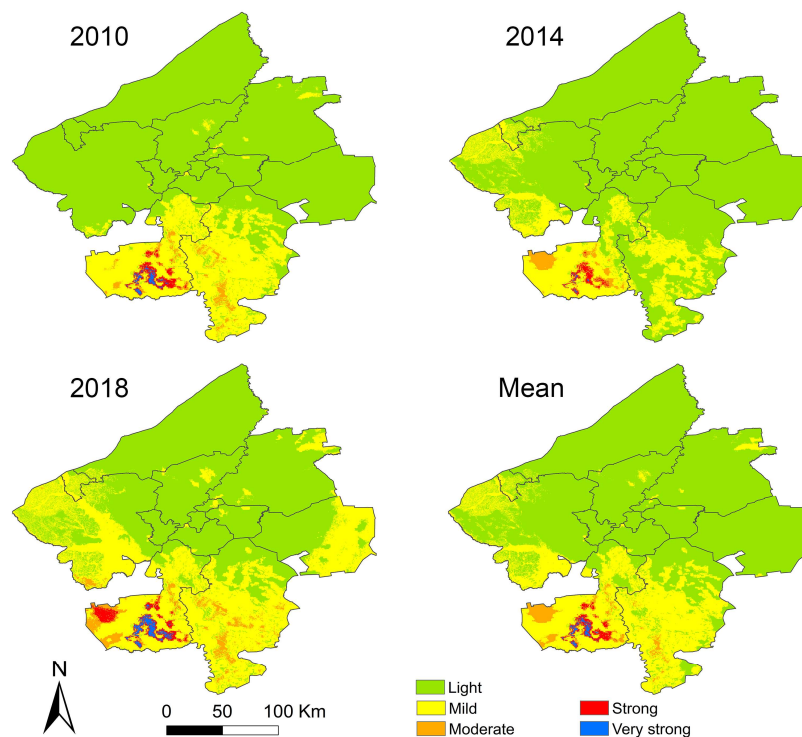


**Figure 5.** Wind erosion grade distribution in the northern Songnen Plain in 2010, 2014, and 2018.

### 3.3. Ecological Effects

This study combined the analysis results of the soil samples with the wind erosion modulus at the sampling sites to analyze the effects of wind erosion on soil physicochemical properties. To this end, we obtained the longitude and latitude coordinates of 56 sampling points, and according to the change of wind erosion at these sampling points in 2010, 2014, and 2018 we established whether they were subject to erosion increase or decrease. According to the soil types (chernozem or aeolian sandy soil) and wind erosion variation (increase or decrease), the soil samples were divided into four categories, and the average values of ecological effects were calculated (Table 2). The clay and silt content in the area with increased wind erosion was lower than in the area with decreased wind erosion, indicating that wind erosion can lead to the loss of fine soil particles [42]. In the regions with increased wind erosion, the contents of soil organic carbon (SOC), soil organic matter (SOM), and total nitrogen (TN) in the topsoil all decreased. In addition, the  $\text{CaCO}_3$  content and pH of the two soil types in the regions with intensified wind erosion increased, which may be one reason for salinization. Soil erodibility refers to the sensitivity of soil to erosion. Generally, soil with high erodibility is more susceptible to erosion than soil with low erodibility [43]. According to the soil mechanical composition, SOM, and  $\text{CaCO}_3$  contents, the soil erodibility factor ( $EF$ ) was calculated.  $EF$ s in the regions with increased wind erosion were higher, indicating that the soil was more vulnerable to erosion.

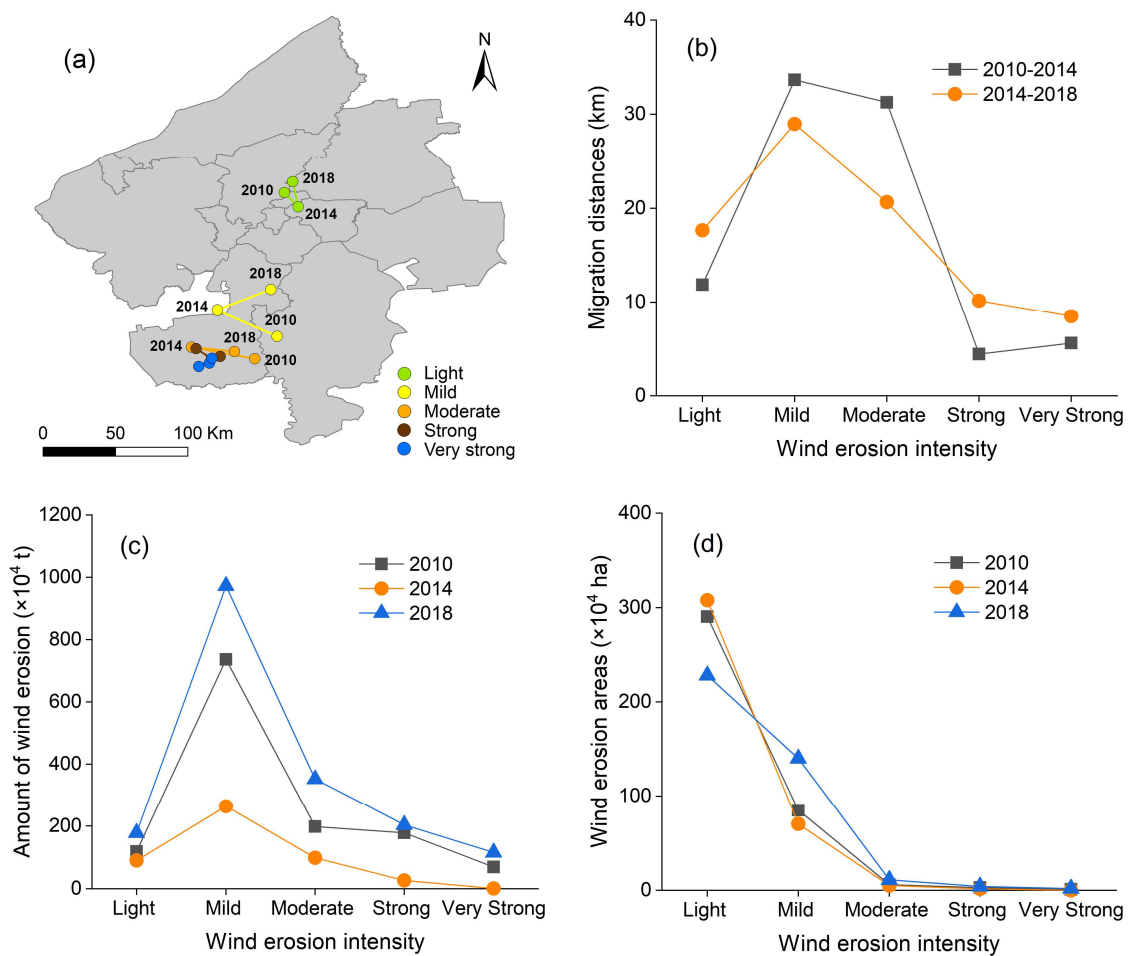


**Figure 6.** Gravity center migration (a), and characteristics of different grades of wind erosion (b–d).

**Table 2.** Changes in soil physicochemical properties in areas with increased and decreased wind erosion.

|                          | C+ <sup>1,3</sup> | C–     | A+     | A– <sup>2,4</sup> |
|--------------------------|-------------------|--------|--------|-------------------|
| SOC (%)                  | 2.864             | 3.119  | 0.984  | 1.139             |
| SOM (%)                  | 4.938             | 5.377  | 1.696  | 1.964             |
| TN (%)                   | 0.177             | 0.221  | 0.073  | 0.090             |
| Sand (0.02–2 mm) (%)     | 49.340            | 42.017 | 74.185 | 64.932            |
| Silt (0.002–0.02 mm) (%) | 44.541            | 50.035 | 22.658 | 31.598            |
| Clay (<0.002 mm) (%)     | 6.121             | 7.948  | 3.158  | 3.474             |
| CaCO <sub>3</sub> (%)    | 3.275             | 1.362  | 0.768  | 0.563             |
| pH                       | 7.45              | 7.29   | 6.29   | 6.09              |
| EF                       | 0.387             | 0.371  | 0.586  | 0.551             |

<sup>1</sup> C represents chernozem soil; <sup>2</sup> A represents aeolian sandy soil; <sup>3</sup> (+) represents increased wind erosion; <sup>4</sup> (–) represents decreased wind erosion. There were 18 samples with increased wind erosion and 7 with decreased wind erosion in the aeolian sandy soils. In chernozem soils, there were 28 samples with increased wind erosion and 3 with decreased wind erosion.

### 3.4. Climatic Effects

Wind erosion in the northern Songnen Plain is positively correlated with wind factors (Figure 7). Wind erosion increased with wind force. Spring is the primary season for wind erosion due to the stronger wind force, indicating it is necessary to monitor the wind speed in spring in the study area and take effective measures amid higher wind speeds. In general, precipitation is negatively correlated with wind erosion (Figure 8). Heavier rainfall led to a smaller amount of wind erosion. Although the rainfall in spring in the study area is not low, the wind erosion in some regions is still intense due to strong wind and uneven rainfall distribution. The wind force is weak in summer and autumn, and the wind erosion is generally light. Temperature is another important factor affecting wind erosion. Results show the temperature in each season is positively correlated with wind erosion. The higher temperature is accompanied by stronger wind erosion, indicating a relationship between them (Figure 9). When the average temperature in spring is higher than 12.5 °C, the wind erosion amount increases rapidly, suggesting that prevention and control measures against wind erosion should be strengthened. In sum, in the northern Songnen Plain, wind erosion is correlated positively with wind force and temperature, and negatively with precipitation.

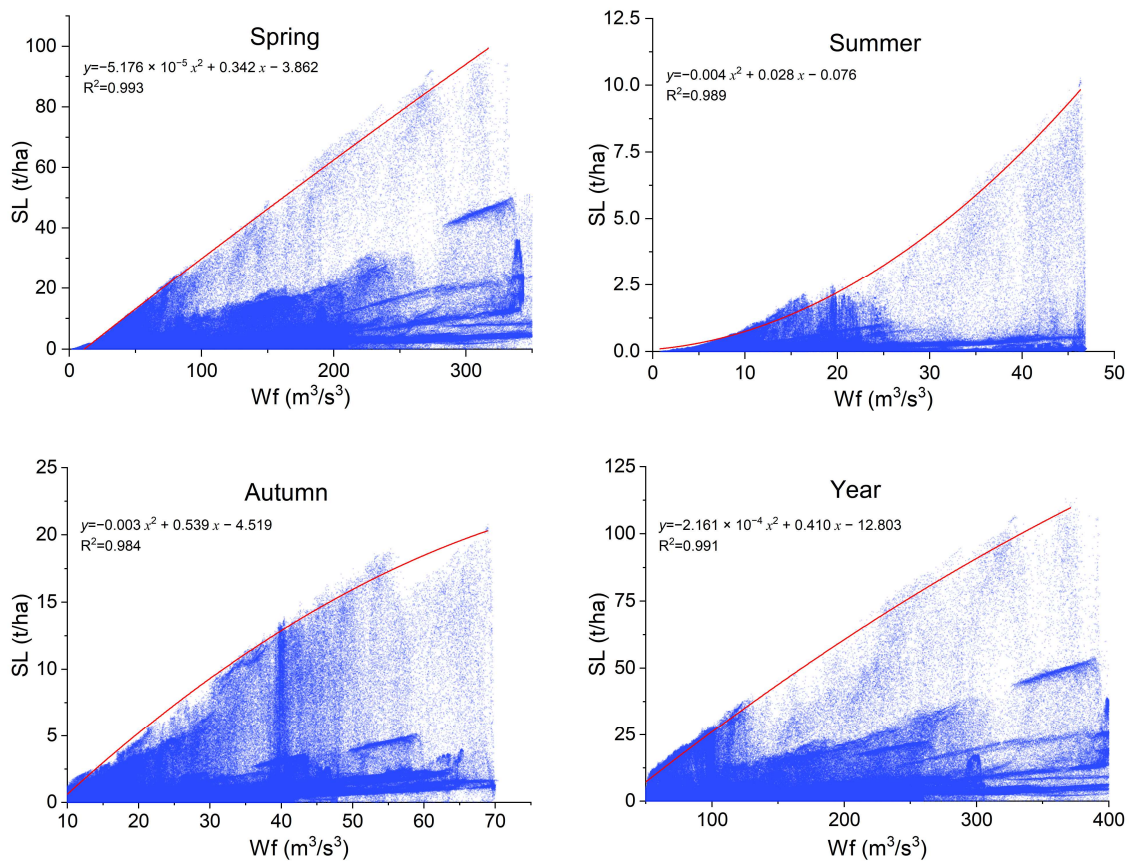


**Figure 7.** Constraint relationship between wind force and wind erosion. Each dot is a 6.25 ha (250 m × 250 m) quadrat.

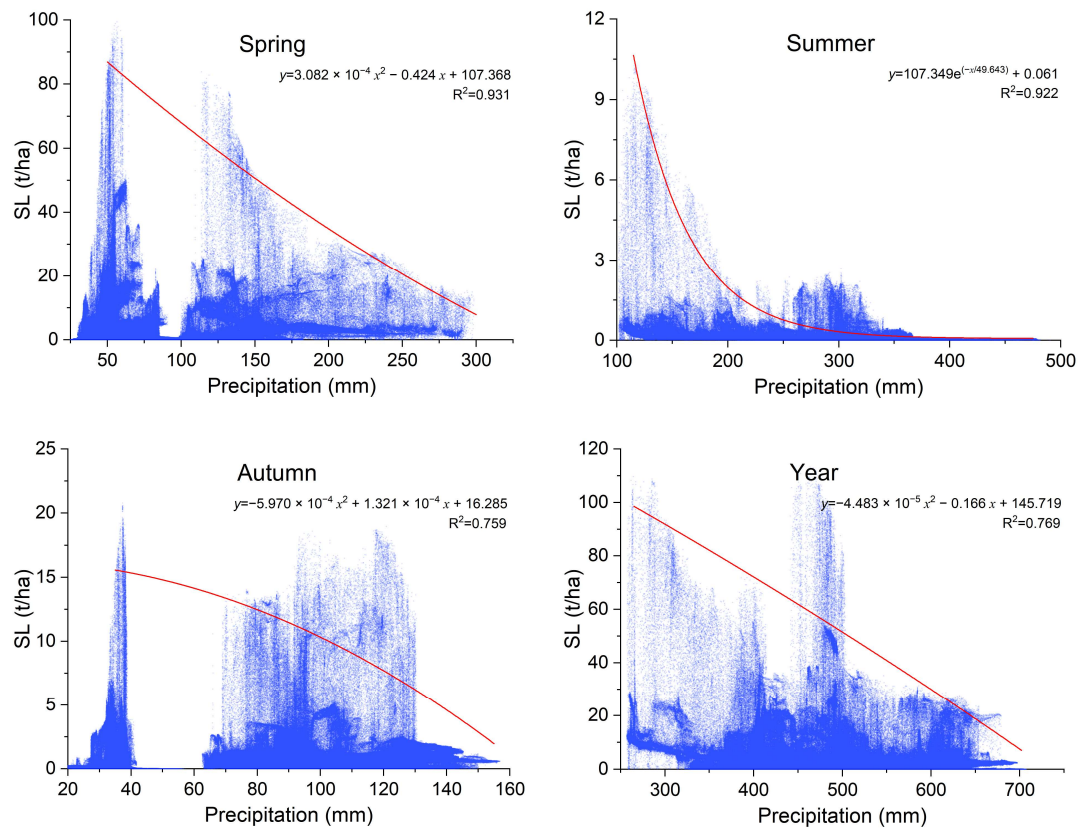


Figure 8. Constraint relationship between precipitation and wind erosion. Each dot is a 6.25 ha (250 m × 250 m) quadrat.

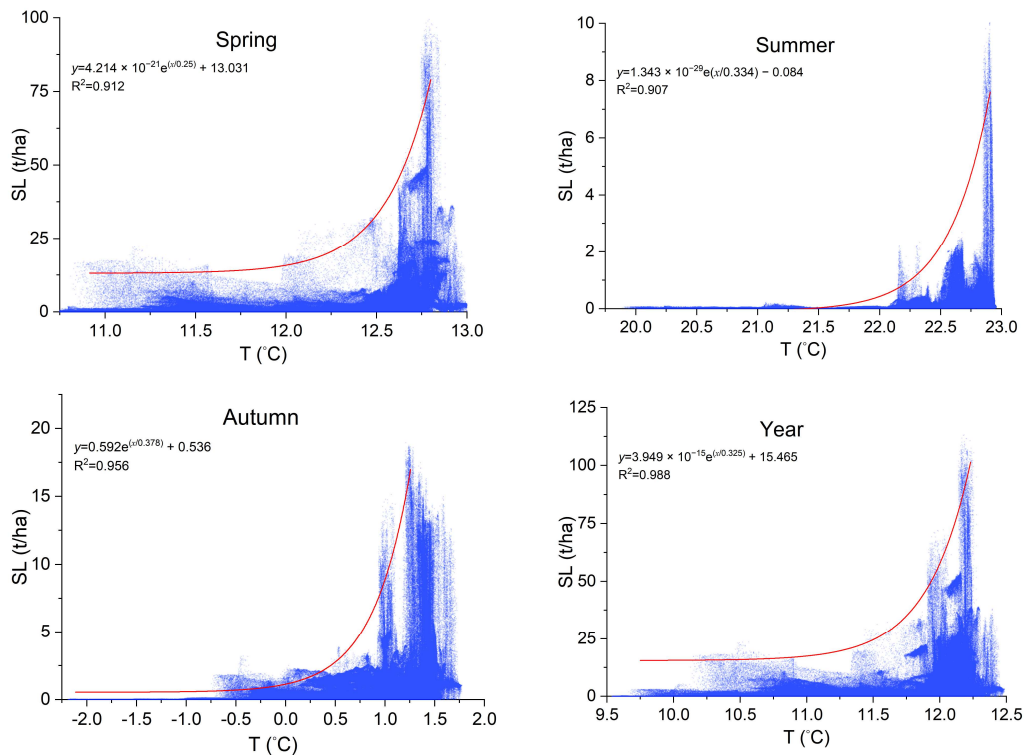
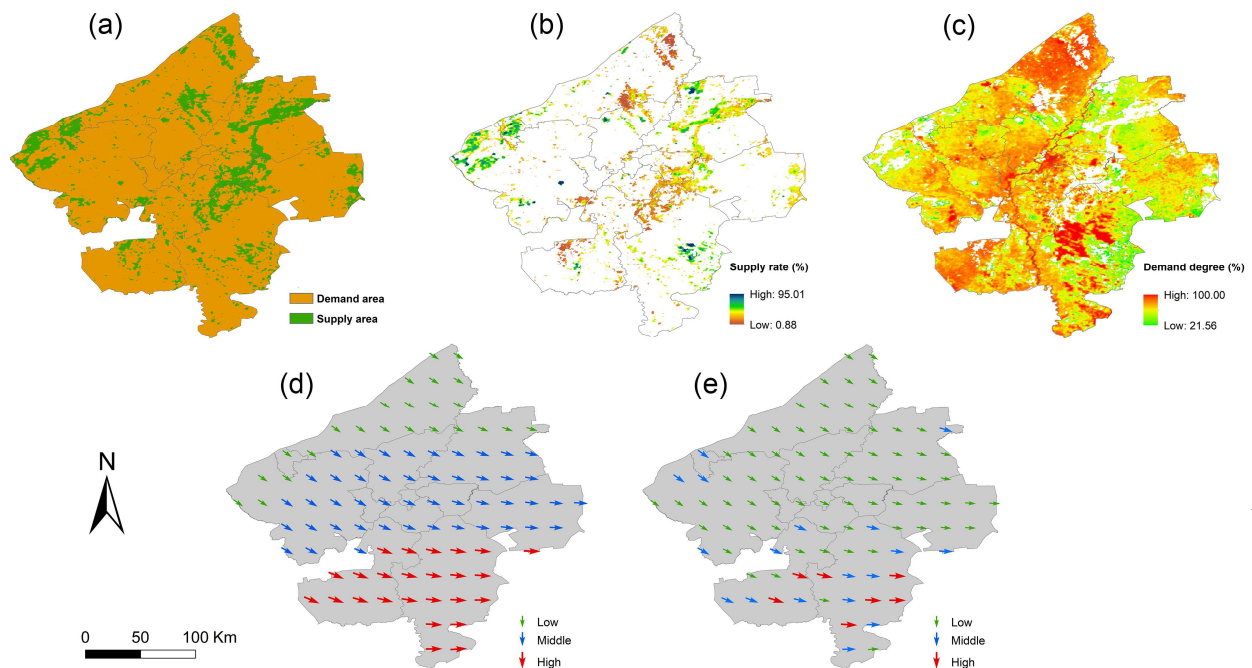


Figure 9. Constraint relationship between temperature and wind erosion. Each dot is a 6.25 ha (250 m × 250 m) quadrat.

### 3.5. Windbreak and Sand-Fixation Service Function

Figure 10 shows the spatial distribution of the windbreak and sand-fixation service function in the northern Songnen Plain. The windbreak and sand-fixation service supply and demand regions in the study area are clearly staggered (Figure 10a). The area of the demand region is much larger than that of the supply region. Most demand areas have higher demand degrees of windbreak and sand-fixation service (Figure 10c). The supply rates in the northeast and central regions are higher (Figure 10b) because the vegetation in these regions is relatively lush and plays a significant role in windbreak and sand-fixation. The windbreak and sand-fixation service in the study area flows from northwest to southeast and east (Figure 10d). The flow velocities and flow volumes in both Tailai and Durbert Mongolia are higher than in other regions, so the supply of windbreak and sand-fixation services should be strengthened in Tailai and Durbert Mongolia. In other regions, such as Longjiang, Fularji, and Lindian, it would be necessary to combine the supply of windbreak and sand-fixation services with a differentiated soil erosion control plan. For example, windbreak forests or farmland protection forests should be built in regions with higher flow velocity to reduce wind speed. Regions with higher flow volume should be converted from farmland to forests and grasslands. The regions with the most severe wind erosion should be comprehensively controlled. Thus, the connection of ecological environment construction between regions should be strengthened to achieve mutual promotion and sustainable development of upstream and downstream regions.



**Figure 10.** Windbreak and sand-fixation service function in the northern Songnen Plain. (a) The supply regions and demand regions; (b) the supply rate; (c) the demand degree; (d) the flow direction (arrow direction) and flow velocity (arrow color and size); and (e) the flow volume (arrow color and size). For panels (a–c), a spatial resolution of  $250 \text{ m} \times 250 \text{ m}$  is used. For panels (d,e), a  $20 \text{ km} \times 20 \text{ km}$  spatial resolution is adopted.

## 4. Discussion

This study analyzes the dynamic temporal and spatial distribution of wind erosion in the northern Songnen Plain using the RWEQ model. The results show that wind erosion in the south and southwest is relatively severe, consistent with our field sampling survey results. The Siberian High forms a robust southwest wind every spring with the highest speed of 13–16 m/s [17,44]. Meanwhile, rainfall in the study area is uneven. The west and

north areas are adjacent to the Great Khingan Mountains, with much rainfall, while others have slight rainfall and extensive evaporation [30]. Moreover, freezing and thawing cycles increase soil porosity, weaken soil cohesion, and aggravate wind erosion [45]. Excessive reclamation and inappropriate land management have caused severe soil erosion in some areas [46], an important driving factor of wind erosion.

Analyzing the soil erosion in Songnen Plain by radionuclide  $^{137}\text{Cs}$  showed that the average erosion rate was over 3 mm/a [15], and the erosion rate in some areas reached 4.64 mm/a, consistent with our research results. This study shows that the average erosion rate only caused by wind erosion in the study area is 2.38 mm/a, and the average erosion rate in the severe wind erosion area achieves 6.39 mm/a. Thus, these pieces of information point to the conclusion that the primary erosion type in the northern Songnen Plain is wind erosion. In addition, the mild wind erosion spread to the black soil area near Lindian county in 2018, the typical black soil zones in Northeast China, affecting the black soil eco-environment and food security. Most research on black soil degradation in Northeast China focused on water [47–49] and freeze–thaw [21,50] erosion in the past. Unfortunately, wind erosion has also begun to ravage this fertile farmland in recent years. We call on more scholars to pay attention to black soil wind erosion and to plan wind erosion prevention strategies.

Changes in physicochemical properties and spatial distribution patterns of soil caused by wind erosion are the important causes of land desertification [18]. Research has showed that arid climatic conditions were not conducive to the enrichment of soil organic matter [51], leading to the vulnerability of SOC to wind erosion [52], which is consistent with our research results. This study shows that the SOC content with increased wind erosion is 10.90% lower than that with decreased wind erosion. In addition, TN content decreased,  $\text{CaCO}_3$  content and pH increased, and coarse soil particles increased (Table 2), indicating that soil physicochemical properties were seriously affected by wind erosion. The effects of wind erosion on different type, temperature, and latitude soils were similar, whether in the Tibetan Plateau at high altitudes [53] or New Mexico at low latitudes [54]. The evaporation of surface water in most wind erosion regions is intense, accumulating groundwater salt on the topsoil with the rise of capillary water, finally causing an increase in ion concentration [55]. Although wind erosion decreases the SOM content, the contents of  $\text{Ca}^{2+}$ ,  $\text{Mg}^{2+}$ , and  $\text{Na}^+$  will not decrease, which is the main reason for slight soil salinization in some regions in the northern Songnen Plain [56]. Wind erosion also affects soil  $\text{CO}_2$  and  $\text{CH}_4$  fluxes, two crucial indicators of soil carbon migration and the carbon pool cycle in terrestrial ecosystems [57]. In some regions with severe wind erosion, excessive fertilizer improves soil fertility. However, adding exogenous N will increase soil  $\text{CO}_2$  and  $\text{CH}_4$  fluxes, which aggravates soil nutrient loss and causes soil structural degradation [58,59].

Temperature, rainfall, and wind force are essential factors affecting wind erosion in the Songnen Plain. From March to November 2018, the average temperature in the northern Songnen Plain was 11.17 °C, 1.33 °C higher than 9.84 °C in 2010. According to the United Nations Framework Convention on Climate Change (UNFCCC), a temperature rise of 1.5 °C significantly increases the risk and impact of climate change [60]. The temperature in the northern Songnen Plain has continued to rise close to the critical value, which will lead to an increase in the extent of sandy areas. In addition, drought is crucial to the formation of wind erosion. In the past 35 years, severe drought in Northeast China has intensified and gradually expanded to the north [46], and about 70% of arable land has suffered from severe drought [13]. Our research shows that from 2010 to 2018, the extreme wind erosion area in the northern Songnen Plain increased by 96.19 km<sup>2</sup> and gradually moved to the northeast, consistent with the increasing drought trend. The reduction of autumn precipitation led to the expansion of wind erosion from spring to spring and autumn. Fortunately, most of the local areas are mainly planted with corn crops, which significantly reduces the intensity of wind erosion in autumn.

Assessing the ecosystem services against wind erosion is a very complex task that should integrate the role of natural and social factors [61]. This study only uses the

vegetation index to assess the windbreak and sand-fixation service function. Although this method may be very imprecise in the assessment of the windbreak and sand-fixation function, the results help promote people's understanding of the problems posed by wind erosion to ecosystems and provide intuitive display information for planning wind erosion prevention strategies. When vegetation coverage is lower than 20%, wind erosion will increase sharply with the decrease of vegetation coverage [62]. Therefore, in this study, 20% is used as the vegetation coverage threshold to calculate the ecosystem service function. Our results show that 14.02% of the land area (5396 km<sup>2</sup>) in the study area would be the supply area for windbreak and sand-fixation service flow, consistent with the 10.4% forest coverage rate calculated by the local government [63]. Figure 10 indicates that the southern region, with intense wind erosion, lacks vegetation coverage, there is a high demand degree for windbreak and sand-fixation services. According to the flow direction of the windbreak and sand-fixation service flow from northwest to east, strengthening the windbreak and sand-fixation measures in Longjiang and Tailai will play a vital role in the wind erosion control in the northern Songnen Plain.

The aggravation of wind erosion will affect the development of local agricultural economies and cause severe ecological and environmental risks. Therefore, soil erosion control and sustainable land management are urgent. The following three methods can help relevant departments to plan effective wind erosion prevention strategies: (1) Develop multiple wind erosion prevention measures in parallel. Stubble and straw mulching can significantly reduce the surface wind speed, potential water evaporation, and moisture exchange capacity at the soil-atmosphere interface [64]. A shelter belt is vital to prevent dry areas from sandstorm disasters, but a certain degree of porosity (20–50%) should be guaranteed [65]. In addition, less or no tillage is an effective way to protect the soil [66,67]. In sum, measures including stubble, straw mulch, protective forests, and no-tillage shall be taken in the study area to control wind erosion comprehensively. (2) Promote multi-party collaboration. Areas subject to relatively severe wind erosion are mainly distributed in Longjiang, Tailai, and Durbert Mongolia. From 2010 to 2018, the wind erosion gravity center continually moved to the northeast. Therefore, it is necessary to strengthen the cooperation between these administrative units and then carry out windbreak and sand-fixation services and ecological governance. At the same time, provincial government departments, including Heilongjiang, Jilin, and Inner Mongolia, should strengthen strategic cooperation in environmental protection to provide policy support for effectively controlling the further increase of wind erosion [68]. (3) Improve regional graded prevention and control. Important differences exist in the spatial distribution of wind erosion in the northern Songnen Plain. We propose to focus on controlling wind erosion in Tailai, especially Huanghua Village and Heping Town, and its surrounding areas. In some regions with high demand for windbreak and sand-fixation services, it is necessary to increase vegetation coverage rapidly. In some areas with high supply rates for windbreak and sand-fixation services, the high-quality development of agriculture and animal husbandry can be appropriately improved to increase local agricultural production and income.

## 5. Conclusions

In recent years, wind erosion in the northern Songnen Plain in China has gradually increased, seriously threatening the eco-environment and food production security. The spatiotemporal distribution of wind erosion in the northern Songnen Plain from 2010 to 2018 was analyzed using the RWEQ model. The development trend, ecological effects, and effects factors of wind erosion at the regional scale were assessed using linear trend analysis, gravity center model, and constraint line method comprehensively. Moreover, the relationships among the supply rate, demand degree, and flow volume of windbreak and sand-fixation services were clarified by visualizing the service functions of the ecosystem windbreak and sand-fixation, providing new ideas and suggestions for preventing wind erosion. The wind erosion amount in the study area increased by 50.78% from 2010 to 2018, reaching  $1973.83 \times 10^4$  t. Wind erosion gradually increased from north to south.

Severe wind erosion is distributed in Tailai, with an annual average wind erosion amount of  $637.67 \times 10^4$  t. The wind erosion in the study area has the characteristics of spatiotemporal dynamic changes. The geographical spatial distribution of wind erosion migrated to the northeast, and the areas of every grade of wind erosion gradually expanded except for the light wind erosion. In particular, the area of severe wind erosion increased by 109.15% to  $1.84 \times 10^4$  ha. Long-term wind erosion has changed soil physicochemical properties, decreasing soil nutrient content and coarsening soil. In addition, the wind erosion in the study area has expanded from spring to spring and autumn, which was distinctly associated with meteorological factors. When the average temperature in spring was higher than 12.5 °C, the wind erosion amount increased rapidly. Wind erosion continued to increase and spread, affecting people's production and life, and threatening the adjacent black soil. A total of 85.98% of the study area has become demand region for windbreak and sand-fixation services. Therefore, we propose wind erosion prevention measures for the land use type in the study area, such as multiple wind erosion prevention measures, multi-party collaboration, and regional graded prevention and control. This study provides a basis for wind erosion regional agricultural sustainable development, land production, and water and soil conservation in the northern Songnen Plain.

**Author Contributions:** Conceptualization, J.M. and J.F.; methodology, J.M., Z.W., and J.F.; software, J.M., J.F., and J.R.; investigation, J.M., J.L., Z.S., and J.R.; data curation, J.M., J.L., Z.S., and Y.C.; writing—original draft preparation, J.M.; writing—review and editing, J.M.; visualization, J.M.; supervision, S.G.; project administration, S.G.; funding acquisition, S.G. All authors have read and agreed to the published version of the manuscript.

**Funding:** This research is supported by the National Key Research and Development Program of China (No. 2021YFD1500801).

**Institutional Review Board Statement:** Not applicable.

**Informed Consent Statement:** Not applicable.

**Data Availability Statement:** The data that support the findings of this study are available from the corresponding author upon reasonable request.

**Acknowledgments:** We would like to thank the anonymous reviewers for their helpful remarks.

**Conflicts of Interest:** The authors declare no conflict of interest.

## References

- Jarrah, M.; Mayel, S.; Tatarko, J.; Funk, R.; Kuka, K. A review of wind erosion models: Data requirements, processes, and validity. *CATENA* **2020**, *187*, 104388. [[CrossRef](#)]
- Li, P.; Liu, L.; Wang, J.; Wang, Z.; Wang, X.; Bai, Y.; Chen, S. Wind erosion enhanced by land use changes significantly reduces ecosystem carbon storage and carbon sequestration potentials in semiarid grasslands. *Land Degrad. Dev.* **2018**, *29*, 3469–3478. [[CrossRef](#)]
- Sterk, G. Causes, consequences and control of wind erosion in Sahelian Africa: A review. *Land Degrad. Dev.* **2003**, *14*, 95–108. [[CrossRef](#)]
- Zhang, H.; Peng, J.; Zhao, C.; Xu, Z.; Dong, J.; Gao, Y. Wind speed in spring dominated the decrease in wind erosion across the Horqin Sandy Land in northern China. *Ecol. Indic.* **2021**, *127*, 107599. [[CrossRef](#)]
- Bridges, E.M.; Oldeman, L.R. Global Assessment of Human-Induced Soil Degradation. *Arid Soil Res. Rehab.* **1999**, *13*, 319–325. [[CrossRef](#)]
- Xu, D.; Li, D. Variation of wind erosion and its response to ecological programs in northern China in the period 1981–2015. *Land Use Policy* **2020**, *99*, 104871. [[CrossRef](#)]
- Shi, P.; Yan, P.; Yuan, Y.; Nearing, M.A. Wind erosion research in China: Past, present and future. *Prog. Phys. Geogr.* **2004**, *28*, 366–386. [[CrossRef](#)]
- Yu, X.; Grace, M.; Zou, Y.; Yu, X.; Lu, X.; Wang, G. Surface sediments in the marsh-sandy land transitional area: Sandification in the western Songnen Plain, China. *PLoS ONE* **2014**, *9*, e99715. [[CrossRef](#)]
- Wang, S.; Xu, X.; Huang, L. Spatial and Temporal Variability of Soil Erosion in Northeast China from 2000 to 2020. *Remote Sens.* **2022**, *15*, 225. [[CrossRef](#)]
- Wang, H.; Wan, Z.; Yu, S.; Luo, X.; Sun, G. Catastrophic eco-environmental change in the Songnen Plain, northeastern China since 1900s. *Chinese Geogr. Sci.* **2004**, *14*, 179–185. [[CrossRef](#)]

11. Yang, Y.; Song, G.; Lu, S. Study on the ecological protection redline (EPR) demarcation process and the ecosystem service value (ESV) of the EPR zone: A case study on the city of Qiqihaer in China. *Ecol. Indic.* **2020**, *109*, 105754. [[CrossRef](#)]
12. Yang, Y.; Song, G. Human disturbance changes based on spatiotemporal heterogeneity of regional ecological vulnerability: A case study of Qiqihaer city, northwestern Songnen Plain, China. *J. Clean. Prod.* **2021**, *291*, 125262. [[CrossRef](#)]
13. Wu, L.; Zhang, Y.; Wang, L.; Xie, W.; Song, L.; Zhang, H.; Bi, H.; Zheng, Y.; Zhang, Y.; Zhang, X.; et al. Analysis of 22-year Drought Characteristics in Heilongjiang Province Based on Temperature Vegetation Drought Index. *Comput. Intell. Neurosci.* **2022**, *2022*, 1003243. [[CrossRef](#)] [[PubMed](#)]
14. Wang, X.; Zhao, X.; Zhang, Z.; Yi, L.; Zuo, L.; Wen, Q.; Liu, F.; Xu, J.; Hu, S.; Liu, B. Assessment of soil erosion change and its relationships with land use/cover change in China from the end of the 1980s to 2010. *CATENA* **2016**, *137*, 256–268. [[CrossRef](#)]
15. Wang, H.; Yang, S.; Wang, Y.; Gu, Z.; Xiong, S.; Huang, X.; Sun, M.; Zhang, S.; Guo, L.; Cui, J.; et al. Rates and causes of black soil erosion in Northeast China. *CATENA* **2022**, *214*, 106250. [[CrossRef](#)]
16. Zhao, H.; Zhang, Z.; Wang, C. Actuality, dynamic change and the prevention countermeasure of desertification in the Songnan Plain. *J. Arid Land Resour. Environ.* **2009**, *23*, 107–113.
17. Shen, Y.; Zhang, C.; Wang, X.; Zou, X.; Kang, L. Statistical characteristics of wind erosion events in the erosion area of Northern China. *CATENA* **2018**, *167*, 399–410. [[CrossRef](#)]
18. Guo, Z.; Huang, N.; Dong, Z.; Van Pelt, R.; Zobeck, T. Wind Erosion Induced Soil Degradation in Northern China: Status, Measures and Perspective. *Sustainability* **2014**, *6*, 8951–8966. [[CrossRef](#)]
19. Xie, Y.; Lin, H.; Ye, Y.; Ren, X. Changes in soil erosion in cropland in northeastern China over the past 300 years. *CATENA* **2019**, *176*, 410–418. [[CrossRef](#)]
20. Xin, Y.; Liu, G.; Xie, Y.; Gao, Y.; Liu, B.; Shen, B. Effects of soil conservation practices on soil losses from slope farmland in northeastern China using runoff plot data. *CATENA* **2019**, *174*, 417–424. [[CrossRef](#)]
21. Liu, T.; Xu, X.; Yang, J. Experimental study on the effect of freezing-thawing cycles on wind erosion of black soil in Northeast China. *Cold Reg. Sci. Technol.* **2017**, *136*, 1–8. [[CrossRef](#)]
22. Kong, F.; Nie, L.; Xu, Y.; Rui, X.; He, Y.; Zhang, T.; Wang, Y.; Du, C.; Bao, C. Effects of freeze-thaw cycles on the erodibility and microstructure of soda-saline loessal soil in Northeastern China. *CATENA* **2022**, *209*, 105812. [[CrossRef](#)]
23. Wei, X.; Wu, X.; Wang, D.; Wu, T.; Li, R.; Hu, G.; Zou, D.; Bai, K.; Ma, X.; Liu, Y.; et al. Spatiotemporal variations and driving factors for potential wind erosion on the Mongolian Plateau. *Sci. Total Environ.* **2022**, *862*, 160829. [[CrossRef](#)] [[PubMed](#)]
24. Li, Y.; Liu, W.; Feng, Q.; Zhu, M.; Yang, L.; Zhang, J. Quantitative Assessment for the Spatiotemporal Changes of Ecosystem Services, Tradeoff–Synergy Relationships and Drivers in the Semi-Arid Regions of China. *Remote Sens.* **2022**, *14*, 239. [[CrossRef](#)]
25. Zhang, H.; Gao, Y.; Sun, D.; Liu, L.; Cui, Y.; Zhu, W. Wind Erosion Changes in a Semi-Arid Sandy Area, Inner Mongolia, China. *Sustainability* **2019**, *11*, 188. [[CrossRef](#)]
26. Chi, W.; Zhao, Y.; Kuang, W.; He, H. Impacts of anthropogenic land use/cover changes on soil wind erosion in China. *Sci. Total Environ.* **2019**, *668*, 204–215. [[CrossRef](#)]
27. Dai, Y.; Tian, L.; Zhu, P.; Dong, Z.; Zhang, R. Dynamic aeolian erosion evaluation and ecological service assessment in Inner Mongolia, northern China. *Geoderma* **2022**, *406*, 115518. [[CrossRef](#)]
28. Gao, C.; Wei, C.; Zhang, L.; Han, D.; Liu, H.; Yu, X.; Wang, G. Historical (1880s–2000s) impact of wind erosion on wetland patches in semi-arid regions: A case study in the western Songnen Plain (China). *Aeolian Res.* **2019**, *38*, 13–23. [[CrossRef](#)]
29. Huang, J.; Tagawa, K.; Wang, B.; Wen, J.; Wang, J. Seasonal Surface Runoff Characteristics in the Semiarid Region of Western Heilongjiang Province in Northeast China—A Case of the Alun River Basin. *Water* **2019**, *11*, 557. [[CrossRef](#)]
30. Huang, J.; Wen, J.; Wang, B.; Zhu, S. Numerical analysis of the combined rainfall-runoff process and snowmelt for the Alun River Basin, Heilongjiang, China. *Environ. Earth Sci.* **2015**, *74*, 6929–6941.
31. Lyu, X.; Li, X.; Wang, H.; Gong, J.; Li, S.; Dou, H.; Dang, D. Soil wind erosion evaluation and sustainable management of typical steppe in Inner Mongolia, China. *J. Environ. Manag.* **2021**, *277*, 111488. [[CrossRef](#)] [[PubMed](#)]
32. Vanpelt, R.; Zobeck, T.; Potter, K.; Stout, J.; Popham, T. Validation of the wind erosion stochastic simulator (WESS) and the revised wind erosion equation (RWEQ) for single events. *Environ. Model. Softw.* **2004**, *19*, 191–198. [[CrossRef](#)]
33. Wang, Y.; Xiao, Y.; Xie, G.; Xu, J.; Qin, K.; Liu, J.; Niu, Y.; Gan, S.; Huang, M.; Zhen, L. Evaluation of Qinghai-Tibet Plateau Wind Erosion Prevention Service Based on RWEQ Model. *Sustainability* **2022**, *14*, 4635. [[CrossRef](#)]
34. Scheper, S.; Weninger, T.; Kitzler, B.; Lackóová, L.; Cornelis, W.; Strauss, P.; Michel, K. Comparison of the Spatial Wind Erosion Patterns of Erosion Risk Mapping and Quantitative Modeling in Eastern Austria. *Land* **2021**, *10*, 974. [[CrossRef](#)]
35. Zhu, D.; Xiong, K.; Xiao, H. Multi-time scale variability of rainfall erosivity and erosivity density in the karst region of southern China, 1960–2017. *CATENA* **2021**, *197*, 104977. [[CrossRef](#)]
36. Duan, H.; Wang, T.; Xue, X.; Guo, J.; Wen, X. Spatial-temporal Evolution of Aeolian Desertification and Landscape Pattern in Horqin Sandy Land: A Case Study of Naiman Banner in Inner Mongolia. *Acta Geogr. Sin.* **2012**, *67*, 917–928.
37. Du, B.; Zheng, Q.; Bai, X.; Shi, L.; Shen, X. Research on Evolution Pattern and Spatial Correlation between Economic Development and Environmental Pollution Centers of Gravity. *Sustainability* **2020**, *12*, 8020. [[CrossRef](#)]
38. Hao, R.; Yu, D.; Wu, J.; Guo, Q.; Liu, Y. Constraint line methods and the applications in ecology. *Chin. J. Plant Ecol.* **2016**, *40*, 1100–1109.

39. Jiang, C.; Zhang, H.; Zhang, Z.; Wang, D. Model-based assessment soil loss by wind and water erosion in China's Loess Plateau: Dynamic change, conservation effectiveness, and strategies for sustainable restoration. *Glob. Planet. Chang.* **2019**, *172*, 396–413. [[CrossRef](#)]
40. Xu, J.; Xiao, Y.; Xie, G.; Wang, Y.; Jiang, Y. How to Guarantee the Sustainability of the Wind Prevention and Sand Fixation Service: An Ecosystem Service Flow Perspective. *Sustainability* **2018**, *10*, 2995. [[CrossRef](#)]
41. Hou, Y.; Lü, Y.; Chen, W.; Fu, B. Temporal variation and spatial scale dependency of ecosystem service interactions: A case study on the central Loess Plateau of China. *Landsc. Ecol.* **2017**, *32*, 1201–1217. [[CrossRef](#)]
42. Rajot, J.L.; Alfaro, S.C.; Gomes, L.; Gaudichet, A. Soil crusting on sandy soils and its influence on wind erosion. *CATENA* **2003**, *53*, 1–16. [[CrossRef](#)]
43. Zamani, S.; Mahmoodabadi, M. Effect of particle-size distribution on wind erosion rate and soil erodibility. *Arch. Agron. Soil Sci.* **2013**, *59*, 1743–1753. [[CrossRef](#)]
44. Park, S.; Cho, J.; Park, S.; Koo, J.; Lee, Y. A Possible Linkage between Dust Frequency and the Siberian High in March over Northeast Asia. *Atmosphere* **2021**, *12*, 176. [[CrossRef](#)]
45. Leuther, F.; Schlüter, S. Impact of freeze–thaw cycles on soil structure and soil hydraulic properties. *Soil* **2021**, *7*, 179–191. [[CrossRef](#)]
46. Wang, B.; Zhao, X.; Wang, X.; Zhang, Z.; Yi, L.; Hu, S. Spatial and temporal variability of soil erosion in the black soil region of Northeast China from 2000 to 2015. *Environ. Monit. Assess.* **2020**, *192*, 370. [[CrossRef](#)] [[PubMed](#)]
47. Dai, T.; Wang, L.; Li, T.; Qiu, P.; Wang, J. Study on the Characteristics of Soil Erosion in the Black Soil Area of Northeast China under Natural Rainfall Conditions: The Case of Sunjiagou Small Watershed. *Sustainability* **2022**, *14*, 8284. [[CrossRef](#)]
48. Liu, B.; Xie, Y.; Li, Z.; Liang, Y.; Zhang, W.; Fu, S.; Yin, S.; Wei, X.; Zhang, K.; Wang, Z.; et al. The assessment of soil loss by water erosion in China. *Int. Soil Water Conse. Res.* **2020**, *8*, 430–439. [[CrossRef](#)]
49. Yang, X.M.; Zhang, X.P.; Deng, W.; Fang, H.J. Black soil degradation by rainfall erosion in Jilin, China. *Land Degrad. Dev.* **2003**, *14*, 409–420. [[CrossRef](#)]
50. Ma, Q.; Zhang, K.; Jabro, J.D.; Ren, L.; Liu, H. Freeze–thaw cycles effects on soil physical properties under different degraded conditions in Northeast China. *Environ. Earth Sci.* **2019**, *78*, 321. [[CrossRef](#)]
51. Xu, Z.; Wang, Y.; Jiang, S.; Fang, C.; Liu, L.; Wu, K.; Luo, Q.; Li, X.; Chen, Y. Impact of input, preservation and dilution on organic matter enrichment in lacustrine rift basin: A case study of lacustrine shale in Dehui Depression of Songliao Basin, NE China. *Mar. Pet. Geol.* **2022**, *135*, 105386. [[CrossRef](#)]
52. Chappell, A.; Webb, N.P.; Leys, J.F.; Waters, C.M.; Orgill, S.; Eyres, M.J. Minimising soil organic carbon erosion by wind is critical for land degradation neutrality. *Environ. Sci. Policy* **2019**, *93*, 43–52. [[CrossRef](#)]
53. Zhang, F.; Zhu, B.; Zheng, J.; Xiong, Z.; Jiang, F.; Han, L.; Wang, T.; Wang, M. Soil properties as indicators of desertification in an alpine meadow ecosystem of the Qinghai–Tibet Plateau, China. *Environ. Earth Sci.* **2012**, *70*, 249–258. [[CrossRef](#)]
54. Díaz-Nigenda, E.; Tatarko, J.; Jazcilevich, A.D.; García, A.R.; Caetano, E.; Ruíz-Suárez, L.G. A modeling study of Aeolian erosion enhanced by surface wind confluences over Mexico City. *Aeolian Res.* **2010**, *2*, 143–157. [[CrossRef](#)]
55. Nachshon, U. Cropland Soil Salinization and Associated Hydrology: Trends, Processes and Examples. *Water* **2018**, *10*, 1030.
56. Li, J.; Okin, G.S.; Alvarez, L.; Epstein, H. Effects of wind erosion on the spatial heterogeneity of soil nutrients in two desert grassland communities. *Biogeochemistry* **2008**, *88*, 73–88. [[CrossRef](#)]
57. Yang, Y.; Li, T.; Pokharel, P.; Liu, L.; Qiao, J.; Wang, Y.; An, S.; Chang, S.X. Global effects on soil respiration and its temperature sensitivity depend on nitrogen addition rate. *Soil Biol. Biochem.* **2022**, *174*, 108814. [[CrossRef](#)]
58. Zhao, L.; Du, M.; Du, W.; Guo, J.; Liao, Z.; Kang, X.; Liu, Q. Evaluation of the Carbon Sink Capacity of the Proposed Kunlun Mountain National Park. *Int. J. Environ. Res. Public Health* **2022**, *19*, 9887. [[CrossRef](#)]
59. Stiehl-Braun, P.A.; Hartmann, A.A.; Kandeler, E.; Buchmann, N.; Niklaus, P.A. Interactive effects of drought and N fertilization on the spatial distribution of methane assimilation in grassland soils. *Glob. Chang. Biol.* **2011**, *17*, 2629–2639. [[CrossRef](#)]
60. Mohan, A.; Geden, O.; Fridahl, M.; Buck, H.J.; Peters, G.P. UNFCCC must confront the political economy of net-negative emissions. *One Earth* **2021**, *4*, 1348–1351. [[CrossRef](#)]
61. Boumans, R.; Roman, J.; Altman, I.; Kaufman, L. The Multiscale Integrated Model of Ecosystem Services (MIMES): Simulating the interactions of coupled human and natural systems. *Ecosyst. Serv.* **2015**, *12*, 30–41. [[CrossRef](#)]
62. Borrelli, P.; Panagos, P.; Ballabio, C.; Lugato, E.; Weynants, M.; Montanarella, L. Towards a Pan-European Assessment of Land Susceptibility to Wind Erosion. *Land Degrad. Dev.* **2016**, *27*, 1093–1105. [[CrossRef](#)]
63. Qiqihar Municipal People's Government Home Page. Available online: [http://www.qqhr.gov.cn/News\\_showNews.action?messagekey=176351](http://www.qqhr.gov.cn/News_showNews.action?messagekey=176351) (accessed on 5 June 2019).
64. Çarman, K.; Gür, K.; Marakoğlu, T. Wind Erosion Risk in Agricultural Soils under Different Tillage Systems in the Middle Anatolia. *Selcuk J. Agric. Food Sci.* **2018**, *32*, 355–360. [[CrossRef](#)]
65. Webb, N.P.; McCord, S.E.; Edwards, B.L.; Herrick, J.E.; Kachergis, E.; Okin, G.S.; Van Zee, J.W. Vegetation Canopy Gap Size and Height: Critical Indicators for Wind Erosion Monitoring and Management. *Rangel. Ecol. Manag.* **2021**, *76*, 78–83. [[CrossRef](#)]
66. Abdalla, K.; Chivenge, P.; Ciais, P.; Chaplot, V. No-tillage lessens soil CO<sub>2</sub> emissions the most under arid and sandy soil conditions: Results from a meta-analysis. *Biogeosciences* **2016**, *13*, 3619–3633. [[CrossRef](#)]

67. Van Thuyet, D.; Van Do, T.; Sato, T.; Thai Hung, T. Effects of species and shelterbelt structure on wind speed reduction in shelter. *Agrofor. Syst.* **2014**, *88*, 237–244. [[CrossRef](#)]
68. Wang, G.; Zhang, H. Spatial Flow and Radiation Effect of Sand-fixing Service in Northwest Liaoning Province. *J. Ecol. Rural Environ.* **2023**, *39*, 52–59.

**Disclaimer/Publisher's Note:** The statements, opinions and data contained in all publications are solely those of the individual author(s) and contributor(s) and not of MDPI and/or the editor(s). MDPI and/or the editor(s) disclaim responsibility for any injury to people or property resulting from any ideas, methods, instructions or products referred to in the content.